



**HAL**  
open science

## Impact of Aging on Copper Isotopic Composition in the Murine Brain

Esther Lahoud, Frédéric Moynier, Tu-Han Luu, Brandon Mahan, Marie Le Borgne

► **To cite this version:**

Esther Lahoud, Frédéric Moynier, Tu-Han Luu, Brandon Mahan, Marie Le Borgne. Impact of Aging on Copper Isotopic Composition in the Murine Brain. *Metallomics*, 2024, 16 (5), pp.mfae008. <10.1093/mtomcs/mfae008>. <hal-04893528>

**HAL Id: hal-04893528**

**<https://hal.science/hal-04893528v1>**

Submitted on 17 Jan 2025

**HAL** is a multi-disciplinary open access archive for the deposit and dissemination of scientific research documents, whether they are published or not. The documents may come from teaching and research institutions in France or abroad, or from public or private research centers.

L'archive ouverte pluridisciplinaire **HAL**, est destinée au dépôt et à la diffusion de documents scientifiques de niveau recherche, publiés ou non, émanant des établissements d'enseignement et de recherche français ou étrangers, des laboratoires publics ou privés.



HAL Authorization

## Impact of Aging on Copper Isotopic Composition in the Murine Brain

1

2 Esther Lahoud<sup>1</sup>, Frédéric Moynier<sup>1</sup>, Tu-Han Luu<sup>1</sup>, Brandon Mahan<sup>2</sup>, Marie Le Borgne<sup>3</sup>

3 <sup>1</sup>Université Paris Cité, Institut de Physique du Globe de Paris, 1 rue Jussieu 75005 Paris, France,

4 [moynier@ipggp.fr](mailto:moynier@ipggp.fr)

5 <sup>2</sup>School of Geography, Earth and Atmospheric Sciences, The University of Melbourne, Australia

6 <sup>3</sup> Université Paris Cité, LVTS, Inserm U1148, F-75018 Paris, France.

7

8

9 **Key words:** aging, copper isotopes, biomarker, Alzheimer's disease, metallomics, MC-ICP-MS

10

11

### 12 **Abstract**

13 Aging is the main risk factor for Alzheimer's disease (AD). AD is linked to alterations in metal  
14 homeostasis and changes in stable metal isotopic composition can occur, possibly allowing the latter  
15 to serve as relevant biomarkers for potential AD diagnosis. Copper stable isotopes are used to  
16 investigate changes in Cu homeostasis associated with various diseases. Prior work has shown that  
17 in AD mouse models, the accumulation of <sup>63</sup>Cu in the brain is associated with the disease's  
18 progression. However, our understanding of how the normal aging process influences the brain's  
19 isotopic composition of copper remains limited. In order to determine the utility and predictive power  
20 of Cu isotopes in AD diagnostics; we aim - in this study - to develop a baseline trajectory of Cu  
21 isotopic composition in the normally aging mouse brain. We determined the copper concentration  
22 and isotopic composition in brains of 30 healthy mice (WT) ranging in age from 6 to 12 months, and  
23 further incorporate prior data obtained for 3-month-old healthy mice; this range approximately  
24 equates to 20-50 years in human equivalency. A significant <sup>65</sup>Cu enrichment has been observed in the  
25 12-month-old mice compared to the youngest group, concomitant with an increase in Cu

26 concentration with age. Meanwhile, literature data for brains of AD mice display an enrichment in  
27  $^{63}\text{Cu}$  isotope compared to WT. It is acutely important that this baseline enrichment in  $^{65}\text{Cu}$  is fully  
28 constrained and normalized against if any coherent diagnostic observations regarding  $^{63}\text{Cu}$   
29 enrichment as a biomarker for AD are to be developed.

30

31

32

### 33 1. Introduction

34 The process of aging provokes wide-ranging effects on the brain, involving various cellular and  
35 molecular changes. Mitochondrial dysfunctions in brain cells lead to a decline in energy metabolism  
36 efficiency. DNA repair mechanisms become compromised resulting in increased genomic instability.  
37 Furthermore, there is an accumulation of soluble (and sometimes neurotoxic) protein precursors [1],  
38 misfolded and aggregated proteins, dysfunctional organelles and elevated levels of oxidative stress  
39 [2]. Numerous studies have established a direct association between oxidative stress, aging and  
40 cognitive decline in humans [3-7]. The progressive increase in oxidative stress during normal aging  
41 is attributed to the imbalance between the production of reactive oxygen species and the ability of  
42 cellular antioxidant defense systems to counteract them.

43 Additionally, neuro-inflammation is a hallmark of the aging brain. Senescent glial cells,  
44 and the infiltration of immune cells into the brain contribute to a chronic state of neuro-inflammation  
45 (see fig1). This process is characterized by elevated levels of pro-inflammatory cytokines and a  
46 decline in anti-inflammatory compounds [8, 9]. Chronic neuro-inflammation not only promotes  
47 neurodegeneration but also accelerates the overall aging process of the brain [10].

48 Aging is recognized as the primary risk factor for neurodegenerative diseases, including  
49 Alzheimer's disease (AD) [11, 12]. Alzheimer's disease is a global health concern, currently affecting  
50 50 millions of individuals worldwide, with an estimated increase to nearly 113 million by 2050 [12,  
51 13]. It is the fifth leading cause of death in high income countries [14, 108].

52           At the cellular level, AD is characterized by two major patho-physiological features: the  
53 presence of extracellular amyloid plaques (A $\beta$ -plaques), formed by the agglomeration of the A $\beta$ 42  
54 peptides, and the formation of intracellular neurofibrillary tangles (NFTs), resulting from abnormal  
55 hyperphosphorylation of the tau protein [12, 15-17]. The latter is mainly due to clinical diagnosis *via*  
56 positron emission tomography (PET) imaging, however it is noted that this technique is predicated  
57 on significant deposition of A $\beta$ -plaques to breach the fidelity threshold of current imaging  
58 instrumentation, which are generally unable to detect the soluble A $\beta$  fraction [48-50]. Current *in vivo*  
59 detection methods are invasive and onerous, involving imaging techniques such as positron-emission  
60 tomography (PET) to visualize amyloid- $\beta$  deposits [18], or measuring the levels of amyloid- $\beta$  or tau  
61 proteins in cerebro-spinal fluids [19, 20].

62           During the initial phase of the disease, A $\beta$ -plaques begin to accumulate in the extracellular  
63 space, yet clinical symptoms, including loss of memory, difficulties in performing executive functions  
64 and solving problems, cognitive decline, apraxia may not manifest for up to 20 years [14, 21]. This  
65 asymptomatic/ preclinical stage of the disease holds great significance for the development of early  
66 diagnosis techniques and the optimization of AD treatments.

67           In addition to other neurodegenerative diseases such as Wilson disease, Menkes disease,  
68 Amyotrophic Lateral Sclerosis (ALS) [22 – 24, 109, 110], AD has also been associated with a change  
69 in the metal homeostasis [25 – 27]. Previous works by Moynier et al., (2019, 2020) have produced  
70 evidences that the changes in the metal isotopic composition, of elements like copper serve as relevant  
71 biomarkers for the future diagnosis of AD [28, 42], and there is a growing body of literature that more  
72 generally suggests viability of stable metal isotopes in disease biomarker development [112].

73           Copper plays a crucial role in various biological processes in the brain, functioning as a  
74 cofactor and structural component of several enzymes involved in essential functions. It participates  
75 in redox metabolism, energy metabolism (cytochrome c oxidase), antioxidative defense (Zn,Cu-  
76 superoxide dismutases), iron metabolism (ceruloplasmin), neurotransmitter synthesis (dopamine- $\beta$ -

77 monoxygenase), regulation of inflammation, and neuropeptide synthesis (peptidylglycine- $\alpha$ -  
78 amidating enzyme) (see fig1) [29- 33].

79         The concentration of Cu in the human brain is typically found to be between 3 and 5  $\mu\text{g/g}$   
80 wet weight [34, 35]. Similarly, a mouse brain contains on average 7  $\mu\text{g/g}$  for a female and 4  $\mu\text{g/g}$  for  
81 a male [43]. Copper has two stable isotopes:  $^{63}\text{Cu}$  and  $^{65}\text{Cu}$  with different relative abundances in  
82 nature of 69% and 31%, respectively. Isotopes undergo fractionation due to changes in bonding  
83 environments within the body [27, 37 - 44]. Isotope fractionation is a general term referring to the  
84 process of creating isotopic variability of a particular element among coexisting species or reservoirs  
85 hosting this element [40, 41]. Heavy isotopes tend to accumulate in environments characterized by  
86 stiffest bonds [37, 38, 45]. For instance,  $^{65}\text{Cu}$  binds preferentially to histidine, glutamate and aspartate  
87 [38, 112]. As a result of the fractionation, the isotopic composition of copper differs in organs:  $^{65}\text{Cu}$   
88 accumulates in the brain, liver and kidney whilst  $^{63}\text{Cu}$  is enriched in red blood cells (RBC) and  
89 plasma. Changes in the isotopic composition of copper in body fluids and in different organs have  
90 been used as proxies to identify cancers [46 – 49], liver diseases [50 – 54] and neurogenerative  
91 diseases [24, 28, 38, 40, 42, 55, 56].

92         In AD mice models expressing the amyloid-beta precursor protein (APP), the accumulation  
93 of  $^{63}\text{Cu}$  in the brain has been shown to be related to the progression of the disease [42]. Besides,  
94 nuclear magnetic resonance (NMR) studies have established that Cu (II) ions interact directly with  
95 A $\beta$  forming a Cu (II)-A $\beta$  complex *in vitro* [32, 57 – 62]. Copper might increase the number of  $\beta$ -sheet  
96 and  $\alpha$ -helix structures in amyloid peptides, which could be a cause of  $\beta$ -amyloid aggregation [63].  
97 Copper and Zinc might also be, in healthy individuals, linked with the degradation of soluble A $\beta$  [64].  
98 Amyloid- $\beta$  sequestering copper, the change in bonding environment due to the emergence of protein  
99 aggregates, amyloid plaques (A $\beta$ ) and neurofibrillary tangles (NFT) is a key to understand this shift  
100 in copper isotopic composition in AD brains.

101         However, prior to any of the above mechanistic pathways for Cu isotope fractionation being  
102 identified, it is requisite to first bolster our current understanding regarding the impact of the normal

103 aging process on the isotopic composition of copper in the brain remains limited, such that if present,  
104 this effect can be accounted for in the development of any future biomarker based on stable Cu  
105 isotopes. The objective of this study is to establish a baseline for the changes in Cu isotopic  
106 composition in the brains of normally aging mice, as a proxy for that in humans. We determined the  
107 copper concentration and isotopic composition in a total of 30 mice (15 males and 15 females) aged  
108 6, 9 and 12-months. Our findings reveal that there is no significant difference in the Cu isotopic  
109 composition of male and female mice (i.e. no sex-dependence). Therefore, we combined the data for  
110 all mice in our analysis. We observed that  $^{65}\text{Cu}$  is enriched in the 12-months old mice compared to  
111 the younger age groups, which show no distinguishable difference. Additionally, the overall copper  
112 concentration in the brain tends to increase with age

## 113 2. Materials and Methods

### 114 2.1. Mice. *At Hopital Bichat.*

115 The 30 WT mice used in this study were collected from VTS INSERM 1148, Hopital Bichat, Paris.  
116 All the 30 mice had the same genotype: C57BL/6JRj. The mice were housed in 6 different cages, 5  
117 same-sex mice per cage. The dry food given to the mice has a  $\delta^{65}\text{Cu} = 0.55 \pm 0.01$  (2SD) [43].

### 118 2.2. Sample collection. *At Hopital Bichat.*

119 Mice\_aged 6, 9 and 12-months were euthanized by receiving a lethal dose of ketamine and xylazine,  
120 followed by exsanguination. Throughout their life cycle, mice were all given the same diet -  
121 previously analyzed in Cu isotopic composition- and kept in similar conditions. The brains were  
122 collected directly after death using instruments in stainless steel. The brains were then conserved in  
123 a -20 degrees Celsius freezer.

124 The biological standard used was tuna fish ERM-CE464 (TF ERM-CE464).

### 125 2.3. Digestion and chemical purification *At Institut de physique du Globe de Paris (IPGP)*

126 The dissolution, chemical purification and mass-spectrometry analyses are a close modification of  
127 the protocols established previously [28, 42].

128 **Dissolution.** In polyfluoralkyl (PFA) beakers, whole brain samples and biological standard (TF ERM-  
129 CE464), all at masses around 100mg, were dissolved in a few droplets of H<sub>2</sub>O<sub>2</sub> and concentrated  
130 distilled HNO<sub>3</sub> for a day and a half. Once the dissolution was complete, the beakers were placed  
131 opened on a hot-plate at 120°C overnight.

132 **Copper extraction.** The Cu purification is conducted using anion- exchange chromatography  
133 following a protocol adapted from [65]. The samples are redissolved in 1mL of distilled 7M HCl then  
134 loaded on 1.6 mL of AG-MP1 resin. Matrix elements are taken away by passing 8 mL of 7M HCl  
135 through the resin. The copper is collected in 16 mL of 7M HCl. This procedure is replicated after  
136 evaporation of the acid to ensure pure Cu fractions. The resin is washed following a day-long protocol  
137 alternating three series of rinses with MQ water and HNO<sub>3</sub> 0.5N in between the two replicates. The  
138 copper was extracted from the standard following the same procedure as for the samples. The yield  
139 of Cu is >99%.

#### 140 **2.4. Mass Spectrometry At Institut de physique du Globe de Paris (IPGP)**

141 Copper isotope ratios were determined with multi-collection inductively-coupled-plasma  
142 mass-spectrometers (MC-ICP-MS) at the Institut de Physique du Globe de Paris France. Part of the  
143 samples were analyzed using a Nu-Instrument Sapphire and the other part using a Thermo-Fisher  
144 Neptune. Depending on instrument performance and availability on the day of analyses; no analytical  
145 differences are observed between instrument platforms (figS1; Table1B). The samples were analyzed  
146 between 1 and 5 times each depending on the amount of copper in each sample (Table1B).

147 The sample-standard bracketing (SSB) method was applied and the Cu concentration in the  
148 samples and standards where match within 10%. This method consists in measuring a standard before  
149 and after each sample and using the average of the two standards to normalize the sample ratio  
150 [40,44]. During analytical session, the standard utilized was IPGP-Cu, previously determined to have  
151 a  $\delta^{65}\text{Cu}$  of  $+0.271 \pm 0.006 \text{ ‰}$  (2SE) relative to the NIST SRM 976 [28]. All data herein have been  
152 converted to  $\delta^{65}\text{Cu}$  relative to NIST SRM 976 by adding 0.271.

#### 153 **2.5. Statistical analysis**

154 Statistical analysis were performed using GraphPad Prism.

155

### 156 3. Results

157

#### 158 3.1. Effect of age on the isotopic composition of Cu in the brain

159

160 We incorporated the data from a previous study conducted by Moynier et al., [43] on 3-months  
161 old mice that were bred together with the mice studied here. All data are reported in Table 1A and  
162 1B and displayed in fig2. The isotopic composition of the biological standard (TF ERM-CE464) was  
163 analyzed every 12 samples on both the Nu-Instrument Sapphire and Thermo-Fischer Neptune  
164 instruments. The value obtained ( $0.09 \pm 0.02$ , 2SD, N=4) was consistent within error with the value  
165 reported by [66, 116], ( $0.11 \pm 0.14$ , 2SD) (Table 2). The Cu isotope compositions of all materials are  
166 expressed as the ratio  $^{65}\text{Cu}$  to  $^{63}\text{Cu}$  relative to that of the internationally recognized standards SRM-  
167 976, in per mil (per thousand) notation, or  $\delta^{65}\text{Cu}$ , and have been calculated using the formula:

168

$$169 \quad \delta^{65}\text{Cu} = \left( \frac{\left( \frac{^{65}\text{Cu}}{^{63}\text{Cu}} \right)_{\text{sample}}}{\left( \frac{^{65}\text{Cu}}{^{63}\text{Cu}} \right)_{\text{NIST SRM 976}}} - 1 \right) \times 1000$$

170

171 Two brain samples were analyzed on both instruments to ensure the consistency of the results.  
172 The results obtained were similar within error: brain-1 gave a  $\delta^{65}\text{Cu} = 0.86 \pm 0.06$ ) on the Neptune  
173 and,  $0.90 \pm 0.05$ ) on the Sapphire. Brain-2 has a  $\delta^{65}\text{Cu}$  of  $0.70 \pm 0.08$  on the Neptune, and of  $0.75 \pm 0.06$ )  
174 on the Sapphire.

175 The values of  $\delta^{65}\text{Cu}$  for mice aged 3 to 12 months were analyzed with One-way ANOVA test  
176 ( $p\text{-value} < 0.0001$ ; R squared= 0.4934). Our data were analyzed with Mann-Whitney test for each age  
177 categories as the data are not normally distributed and the number of data is close to 30. Mann-

178 Whitney test: (age 9 vs age 6; p-value = 0,0051); (age 6 vs 12; p-value = <0.0001); (age 3 vs age 6;  
179 p-value = 0.7915, ns); (age 12 vs age 9; p-value = 0,0008) (see fig2A).

180 The results (see fig2A, B, C) reveal a notable evolution in the isotopic composition of copper  
181 as a function of age. Mice aged between 3 and 6 months exhibit a relatively consistent composition  
182 of copper isotopes, with a  $\delta^{65}\text{Cu}$  value of  $0.85\pm 0.23$  (2SD). However, from the age 9 months onwards  
183 (mean:  $\delta^{65}\text{Cu} = 0.98\pm 0.22$  (2SD)) there is a noticeable shift towards heavier copper content and  
184 dispersion of  $\delta^{65}\text{Cu}$  values, particularly evident in the 12 months old mice (mean:  $\delta^{65}\text{Cu} = 1.32\pm 0.61$   
185 (2SD)) (fig2A and 2B). The simple linear regression (fig2C) plotted using the values displayed in  
186 fig2B has a positive slope and shows a linear increase in the values of  $\delta^{65}\text{Cu}$  depending on time. An  
187 un-linear curve showing was plotted as well in fig2C and is also displaying a heavier copper isotopic  
188 composition as a function of age. Taken as a whole, these data strongly suggest that the isotopic  
189 composition of copper undergoes significant changes with age. Specifically, the copper composition  
190 becomes progressively heavier with advancing age. Consequently, the aging process is associated  
191 with a shift in the isotopic composition of copper, particularly in the brain, which demonstrates an  
192 age-dependent increase in the proportion of  $^{65}\text{Cu}$  compared to  $^{63}\text{Cu}$ .

193

### 194 **3.2. Effect of age on copper concentration**

195

196 Several studies in the literature have reported an age-related increase in copper levels in  
197 various organs. In healthy individuals, it has been observed that copper tends to increase with age in  
198 human serum [67, 68]. However, in cortical tissue affected by Alzheimer's disease (AD), the level of  
199 copper is actually decreased [69]. This decrease is believed to be associated with the binding of copper  
200 to senile plaques [70]. Other studies have shown that copper tends to decrease in salivary sediment  
201 and hair samples [71]. In rats aged 15 to 49 weeks, Cu level increase in the serum, kidney, liver and  
202 five distinct parts of the brain (cortex, corpus striatum, hippocampus, midbrain+medulla and

203 cerebellum) [72]. These findings further support the notion of age-dependent changes in copper  
204 amounts across different tissues and species.

205 Copper concentrations aren't the main focus in the study. They are determined as a matter of  
206 comparison with other studies that determine the concentrations the same way. Our objective was to  
207 investigate whether there were any variations in copper concentration within our samples. To  
208 accomplish this, we quantified the copper concentration in each brain sample (n=30). For each  
209 sample, we performed a factor 100 dilution (10 $\mu$ L of sample in 1mL of 0.5N HNO<sub>3</sub>) and measured  
210 the signal in volts obtained on the MC-ICP-MS. Given that the concentration and signal were  
211 precisely known for the standard (NIST SRM 976), we could compute the concentration of copper in  
212 each of the samples. The weight collected for each sample was 100mg $\pm$ 30. The data are in Table 3  
213 and displayed in fig3. The concentrations are given in ppm, equivalent to a concentration given in  
214  $\mu$ g/g. The means were calculated for each age category: mice aged 6 months (mean: C<sub>copper</sub> = 3.73  
215 ppm, 2sd = 2.50, n=10), mice aged 9 months (mean: C<sub>copper</sub> = 4.39 ppm, 2sd = 5.58, n=10), mice aged  
216 12 months (C<sub>copper</sub> = 6.02 ppm, 2sd = 4.56, n=10) (see fig3).

217 We performed a Mann-Whitney test: age 12 vs 9 (p-value = 0,2475, ns) and age 12 vs age 6  
218 (p-value = 0,0089, \*\*). Ordinary one-way ANOVA and 2way ANOVA were not conclusive.  
219 However, we observe a qualitative increasing trend as a function of age. The data obtained for mice  
220 aged 9 months are very disperse compared to 6 and 12 months-old mice (see fig3).

221

222

## 223 **4. Discussion**

### 224 **4.1. Effect of sex on copper isotopic compositions and concentrations**

225

226 Previous studies have demonstrated differences in the isotopic composition of Cu and Fe in  
227 function of sex notably in the serum and red blood cells [28, 73, 74]. In archeological human bones,  
228 Jouen et al., have shown that the isotopic signature is dependent on sex for Cu and Fe [74].

229 Furthermore, several studies have indicated sex-related differences in the development of  
230 neurodegenerative diseases. For instance, men have a higher disposition for Parkinson's disease [75-  
231 77] while women constitute two-thirds of AD patients [78]. Moreover, the progression of the disease  
232 progression appears to be accelerated in men [79]. Although these sex-dependent differences are  
233 known, their underlying causes remain elusive and require further investigation. To better constrain  
234 the sex effect on brain isotopic composition and concentration, we conducted a comparison between  
235 the results obtained for males and females, irrespective of age. However, no significant difference  
236 was observed between the two groups. Furthermore, we further examined the data by plotting the  
237 results for males and females separately in each age category. Even after considering age as a factor,  
238 no notable or statistically significant differences between the sexes were found (see fig4; Table4;  
239 Table 5).

240 We conducted a Mann-Whitney test to compare the  $\delta^{65}\text{Cu}$  values between males and females,  
241 which revealed no statistical difference (p-value = 0.1276). The mean  $\delta^{65}\text{Cu}$  for males was  $0,98\pm 0.48$   
242 (2SD), while for females it was  $1.13\pm 0.67$  (2SD) (see fig4A). Additionally, males and females could  
243 not be statistically differentiated based on copper concentrations (see fig4B).

244 Although there was no significant difference in  $\delta^{65}\text{Cu}$  between males and females, it is worth  
245 noting that the data for females exhibited a slightly broader distribution compared to males.  
246 Furthermore, there is a tendency in the evolution of  $\delta^{65}\text{Cu}$  values between males and females as a  
247 function of time (fig4D), however more samples from future work might drive this further towards  
248 statistical significance. The difference in copper isotopic composition between males and females  
249 tends to increase as a function of time. As reported in the study by Moynier et al., (2019), at age 12,  
250 there was a discernible difference in  $\delta^{65}\text{Cu}$  values between males and females. However, in our study,  
251 it did not reach statistical significance (see fig4C)

252

253 **4.2.  $\delta^{65}\text{Cu}$  decreases after 12 months.**

254 To provide a better understanding of the evolution of  $\delta^{65}\text{Cu}$  with age, we combined our data  
255 with literature [43, 107] (fig5). Moynier et al., (2022) measured 4 brains from healthy mice aged 3  
256 months, Morel et al., (2022) measured 29 brains from mice aged 6, 16 and 24 months. All mice have  
257 the same genotype. The data show an increase in  $\delta^{65}\text{Cu}$  values before 12 months and a decrease after  
258 12 months. Combining the data from Morel et al., (2022) with our data, we could observe that both  
259 data from mice aged 6 months are consistent. Performing Mann-Whitney test for the 6 and 9 months,  
260 p-value = 0.0004, \*\*\*, which is even lower when the data are combined with Morel et al., (2022)  
261 compared to our data alone (p-value = 0.0051). Even if the measurement method and copper  
262 extraction vary slightly between the studies, the results are consistent.

263

#### 264 **4.3. 12 months old WT and AD mice have different brain copper isotopic compositions**

265

266 Combining our data for 12 months old healthy mice with those from Moynier et al. (2019)  
267 [28], we obtained a mean  $\delta^{65}\text{Cu} = 1.32 \pm 0.61$  (2SD) for healthy 12 months-old mice (WT), in our  
268 study. For 12 months-old AD mice (AD), the mean was  $\delta^{65}\text{Cu} = 0.50 \pm 0.29$  (2SD). We also took into  
269 account the  $\delta^{65}\text{Cu}$  values for healthy mice brains reported in Moynier et al., (2019). The data are  
270 statistically differentiable (Mann-Whitney, p-value < 0.01, \*\*). The results (see fig6A; Table 6) show  
271 a decrease in the isotopic composition between WT and AD at 12 months. However, we could only  
272 have five samples for AD mice ages 12 months. Despite the limited data, this difference is considered  
273 robust, as a statistical difference of well over 0.5 per mil is over an order of magnitude larger than  
274 typical analytical precision within this and other studies.

275 This suggests that AD brains are isotopically lighter than healthy ones in terms of copper  
276 isotopes (see fig6B). This is also what is found in literature in the brains of AD and WT humans [42].  
277 This can be explained by the change in bonding environment caused by the appearance of amyloid  
278 plaques and neurofibrillary tangles, as copper directly interacts with  $\text{A}\beta$  [42,57,58, 70]. The new  
279 environment created by the presence of amyloid plaques in the brain might encourage the binding of

280 lighter isotopes and thus generating a shift in the natural isotopic fractionation of copper. Copper  
281 being a redox active metal [25] and Cu (II) ions binding preferentially to A $\beta$  plaques this also could  
282 be a source of explanation for this shift [42,57,58, 70]. Conversely, the presence of Cu (0) has been  
283 detected in AD human brains [80].

284 Normal aging and AD have different signatures in terms of copper concentration as well.  
285 In the literature, it is reported that AD is accompanied by a deficiency in copper in the brain [69,81,  
286 82]. Interestingly, the amount of Cu in aged human brains has been shown to have a negative  
287 correlation with the advance of A $\beta$  plaques [83]. Normally aging individuals tend to have copper  
288 accumulating in the brain as a function of age. Thus, AD and healthy individuals appear to display  
289 different copper signatures regarding copper isotopic composition and copper concentration.

290

#### 291 **4.4. Copper related oxidative stress might be a key to understand normal aging in the brain**

292

293 Oxidative stress is thought to be one of the main causes of aging in mammals [3-6]. In the  
294 brain, the levels of antioxidants are low: it makes it susceptible to oxidative stress induced by the  
295 redox-active nature of Cu [84]. Superoxide dismutases (SODs) are a category of ubiquitous enzymes  
296 representing one of the main antioxidant defense systems against reactive oxygen species (ROS).  
297 SODs catalyze the dismutation reaction of O $_2^{\bullet-}$  to H $_2$ O $_2$  which is then reduced to H $_2$ O by the action  
298 of catalase [85]. The reaction requires alternate reduction and reoxidation of a redox active transition  
299 metal (Cu or Mn). In mammals, there are three isoforms that are all bound to catalytic metals:  
300 intracellular SOD1 or CuZn-SOD, mitochondrial SOD2 or Mn-SOD and extracellular SOD3 [86].  
301 SOD1 is intracellular [87, 88].

302 Warner et al., (1994), have shown, through genetic manipulations increasing CuZn-SOD  
303 activity, a resistance to most forms of oxidative stress [89]. CuZn-SOD deficiency increases the  
304 vulnerability to oxidative stress and thus potentially normal aging. Copper is bound to several  
305 proteins, frequently enzymes, including metallothionein. It has been shown that SOD1 was enriched

306 in  $^{65}\text{Cu}$  relative to the metallothionein (MT) in human cortex [90]. Thus, probably due to specific  
307 catalytic micro-environments, SOD1 seems to be a source of Cu fractionation.

308 The distributions of Cu isotopes between MT and SOD1 in AD patients is also different  
309 compared to healthy patients [90]. CuZn-SOD activity is negatively correlated with age [91] which  
310 might partly explain the increase of ROS in cells and tissues. However, while the activity of the  
311 enzyme seems to decrease with age, its concentration appears to follow the opposite tendency. It was  
312 shown that in the cerebro-spinal fluid (CSF), the concentration of SOD1 tends to increase with age  
313 [111]. As we mentioned, SOD1 binding preferentially  $^{65}\text{Cu}$ , which might explain the increase in  
314  $^{65}\text{Cu}/^{63}\text{Cu}$  ratio in CSF compared to the decrease in the  $^{65}\text{Cu}/^{63}\text{Cu}$  ratio observed in the brain [90]  
315 (fig2). The variations observed in this study and in other studies (fig6) [107] for both  $\delta^{65}\text{Cu}$  values  
316 and Cu concentrations (ppm) as a function of age might be related to SOD1 concentration and activity  
317 during aging and -more generally - to enzymes binding copper in the brain. Further investigations  
318 regarding this aspect would be interesting to understand precisely the mechanisms involved, notably  
319 including the parallel-operating influence of MT and the influence this may have on Cu isotope  
320 composition.

321

#### 322 **4.5. Effect of glial cells and neuroinflammation on copper contents in the brain**

323

324 Astrocytes are a specific type of glial cells in the central nervous system (CNS) that are  
325 reported to have - amongst others - a role in the maintenance of extracellular ion homeostasis [92,  
326 93]. They are key regulators of Cu and Fe in the brain [94 – 96]. Astrocytes express copper  
327 transporter 1 (Ctr1) [97] as well as MT [98] and glutathione (GSH) [99]. Ctr1 is the main copper  
328 transporter in eukaryotic cells and is responsible for copper entrance in the cell [100]. When the brain  
329 ages, astrocytes encounter senescence and their functions become dysregulated [101]. This is thought  
330 to have an impact on the accumulation of debris and especially  $\text{A}\beta$  plaques [102, 103]. Furthermore,  
331 copper has been shown to activate the secretion of inflammatory products such as IL- 6, NO and

332 TNF- $\alpha$  by interacting with microglia [104]. Microglia are as well as astrocytes a type of glial cell and  
333 the main type of immune cell in the brain [105]. Inflammation in the brain promotes the appearance  
334 and development of neurodegenerative diseases [10,106]. Ashraf et al., (2019), demonstrated that  
335 glial senescence may induce differential regional content of metals (Cu, Zn, Fe) [106]. In chronic and  
336 acute inflammatory conditions, copper is reported to be at higher concentrations in the brain. In the  
337 same conditions, labile copper was found to be also at higher concentrations in microglia. It has been  
338 shown in copper-deficient rats that a lack of copper is linked with a sensitivity to acute inflammatory  
339 agents [113]. Copper seems to be implied in the regulation of inflammation in the brain. Moreover,  
340 the copper complex copper*bis*(thiosemicarbazones) ( $\text{Cu}^{\text{II}}$  (at-sm)) was shown to be a potential  
341 therapeutic candidate for strokes and acute brain injuries [114]. This same copper complex has also  
342 been shown to have protective effects in animal models of neurodegenerative diseases such as ALS  
343 and AD [114, 115].  $\text{Cu}^{\text{II}}$  (at-sm) was reported to have an anti-inflammatory action by potentially  
344 restoring the brain copper homeostasis [114]. We propose that the senescence of glial cells, as well  
345 as neuro-inflammation and its peripheral processes during ageing, could be key contributing factors  
346 to understanding the accumulation of copper, and potentially other metals, in the ageing brain, and  
347 therefore hold relevance in understanding the evolution of Cu isotope compositions in the brain as a  
348 function of age as well as potential therapeutic candidates.

349

## 350 5. Conclusions

351 This study has provided evidence that the isotopic composition of copper in the brain  
352 undergoes changes with normal ageing, manifesting an increase in the  $^{65}\text{Cu}/^{63}\text{Cu}$  ratio with age. These  
353 results suggest that the copper isotopic signature becomes progressively heavier as individual ages,  
354 accompanied by a tendency towards Cu accumulation in the aging brain. Notably, we observed a  
355 distinct shift in  $^{65}\text{Cu}/^{63}\text{Cu}$  ratio between healthy and AD model mice at 12 months. While the ultimate  
356 utility of Cu isotopes in AD diagnostics remains to be clear, the present work provides an invaluable  
357 baseline trajectory of Cu isotope compositions in the brain with age. This baseline progression must

358 be well-understood so that it can be deconvolved from other alterations to Cu isotope compositions,  
359 namely the observed light Cu isotope excursion in the AD brain; this is paramount to mechanistically  
360 and statistically isolating a potential biomarker signal induced by the disease. These findings greatly  
361 contribute to the development of a baseline Cu isotope signature associated with normal aging,  
362 enhancing our ability to understand Cu isotope changes induced by neurodegenerative diseases such  
363 as Alzheimer's.

364

## 365 **6. Acknowledgments**

366 We thank Tu-Han Luu for her help with the mass-spectrometers laboratory at IPGP. EL thanks AAT  
367 for fundings. FM thank the ERC for the POC Grant DAI (# 101081580). Parts of this work were  
368 supported by IPGP multidisciplinary program PARI, by Region Île-de-France SESAME Grants no.  
369 12015908, EX047016, and the IdEx Université de Paris grant, ANR-18-IDEX-0001 and the DIM  
370 ACAV+.

## 371 **7. Disclosure statement**

372 The authors have no actual or potential conflicts of interest.

373

## 374 **8. Data availability**

375 The data underlying this article are available in the article and in its online supplementary material.

376

377

## 378 **Figure captions**

379 **Fig1.** The roles of copper in a healthy brain. Made with BioRender.

380

381 **Fig 2.** A.  $\delta^{65}\text{Cu}$  in healthy mouse brain in function of age. Boxes extend from the 25<sup>th</sup> and 75<sup>th</sup>  
382 percentile, the line inside the box represents the median, the whiskers show the minimum and

383 maximum of the values. p-value < 0.001; \*\*, p-value < 0,0001; \*\*\*\*. B.  $\delta^{65}\text{Cu}$  in healthy mouse  
384 brain in function of age. Each point corresponds to the mean for one mouse, n corresponds to the  
385 number of brains measured per age category. C. Simple linear regression for the data displayed in  
386 figure 2B (black full line) with 95% confidence intervals (dotted line),  $R^2= 0.3946$  and quadratic  
387 second order polynome (red full line),  $R^2= 0.5126$ . GraphPad Prism.

388 **Fig 3.** Concentration of copper (ppm) in function of age. Boxes extend from the 25<sup>th</sup> and 75<sup>th</sup>  
389 percentile, the line inside the box represents the median, the whiskers show the minimum and  
390 maximum of the values. p-value < 0.02, \*. GraphPad Prism.

391 **Fig 4.** A, B, C.  $\delta^{65}\text{Cu}$  in function of sex (A), copper concentration in function of sex (B),  $\delta^{65}\text{Cu}$  in  
392 function of sex and age (C). (D) is the evolution of the p-values for unpaired-t tests between males  
393 and females as a function of age,  $R^2 = 0.9988$ . Boxes extend from the 25<sup>th</sup> and 75<sup>th</sup> percentile, the line  
394 inside the box represents the median, the whiskers show the minimum and maximum of the values.

395 **Fig5.**  $\delta^{65}\text{Cu}$  in healthy mouse brain in function of age. Data from (Moynier et al., 2022) and (Morel  
396 et al., 2022) were incorporated to the data from this study. Boxes extend from the 25<sup>th</sup> and 75<sup>th</sup>  
397 percentile, the line inside the box represents the median, the whiskers show the minimum and  
398 maximum of the values. p-value < 0.001, \*\*\*. GraphPad Prism.

399 **Fig 6.** A, B. Isotopic composition of copper in the brain of healthy and AD mice. p-value < 0.001, \*\*  
400 (A), copper isotopic composition of a healthy (green) and Alzheimer brain (red) (B). Boxes extend  
401 from the 25<sup>th</sup> and 75<sup>th</sup> percentile, the line inside the box represents the median, the whiskers show the  
402 minimum and maximum of the values. GraphPad Prism, Bio Render.

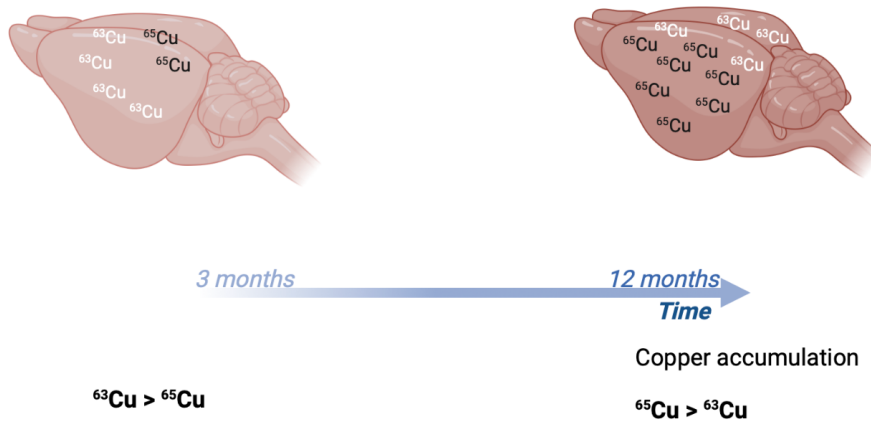
403

404

405

406

407



Graphical

abstract.

420 Made with BioRender.

421

422

423

424

425

426

427

428

429

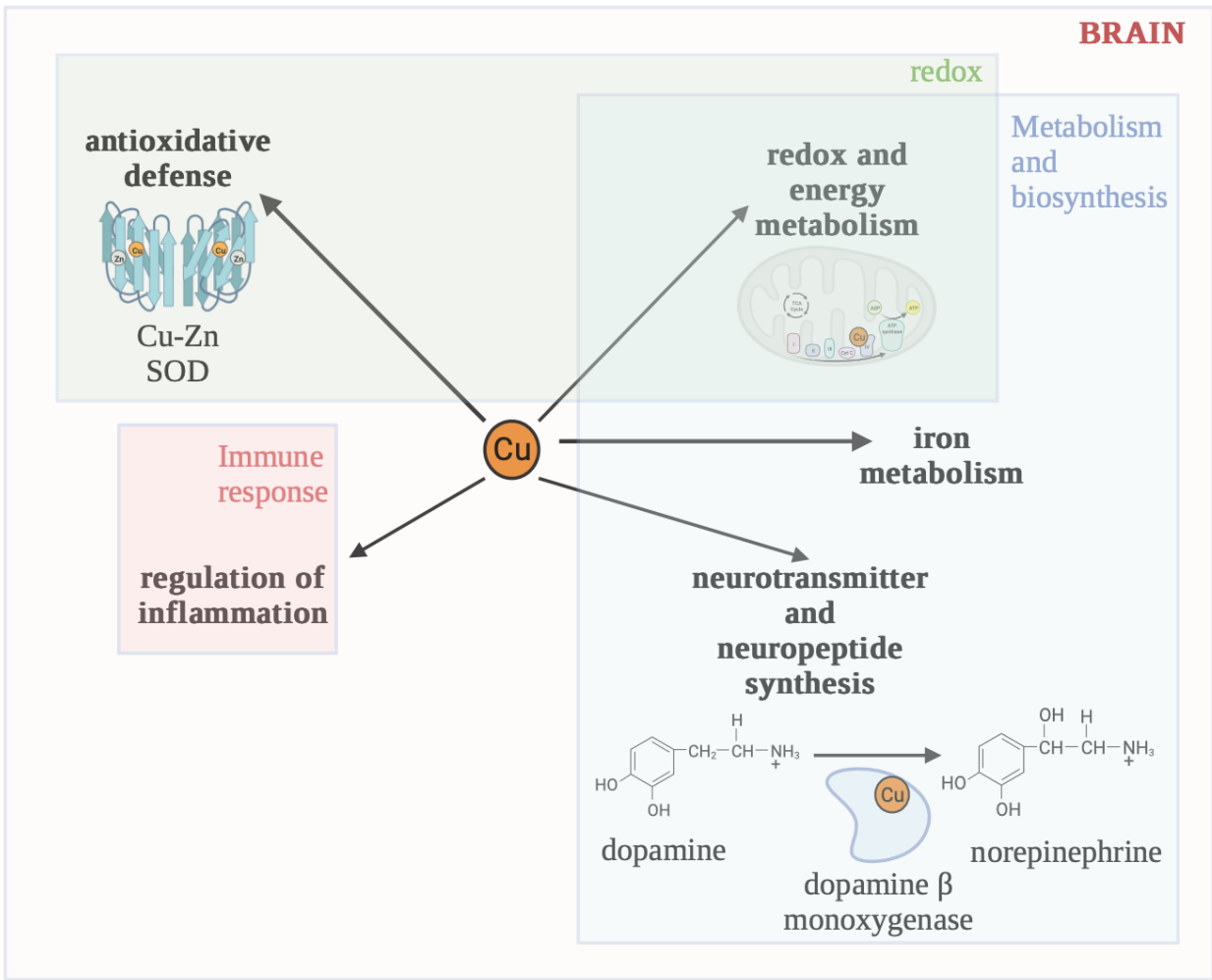
430

431

432

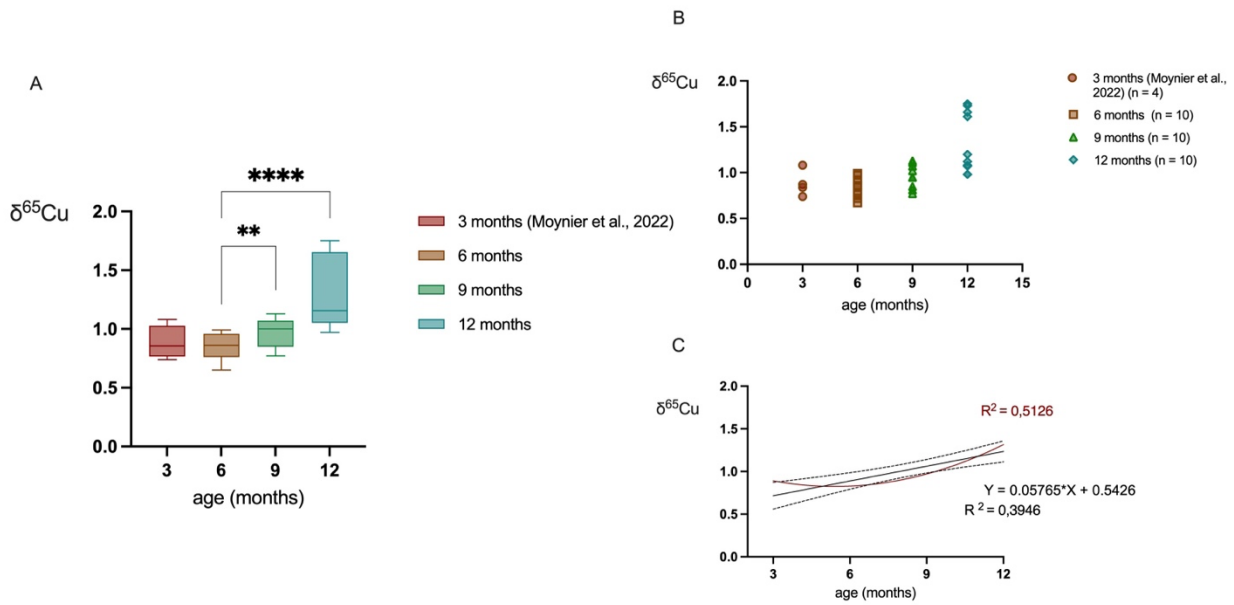
433

434  
435  
436  
437  
438



439  
440  
441  
442  
443  
444

Fig1. The roles of copper in a healthy brain. Made with BioRender.



445

446

447

448 Fig 2. A.  $\delta^{65}\text{Cu}$  in healthy mouse brain in function of age. Boxes extend from the 25<sup>th</sup> and 75<sup>th</sup>

449 percentile, the line inside the box represents the median, the whiskers show the minimum and

450 maximum of the values. p-value < 0.001; \*\*, p-value < 0,0001; \*\*\*\*. B.  $\delta^{65}\text{Cu}$  in healthy mouse

451 brain in function of age. Each point corresponds to the mean for one mouse, n corresponds to the

452 number of brains measured per age category. C. Simple linear regression for the data displayed in

453 figure 2B (black full line) with 95% confidence intervals (dotted line),  $R^2 = 0.3946$  and quadratic

454 second order polynome (red full line),  $R^2 = 0.5126$ . GraphPad Prism.

455

456

457

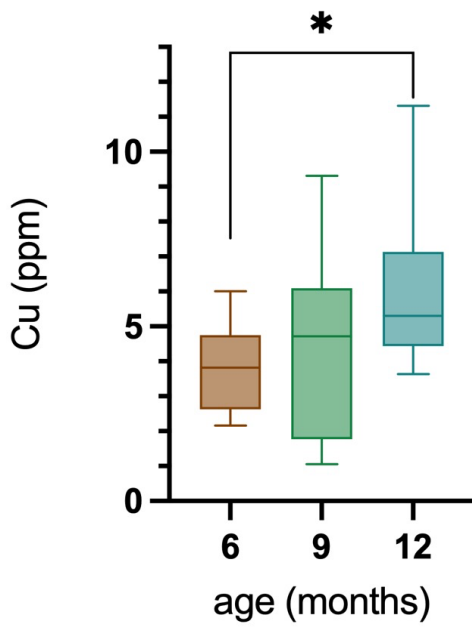
458

459

460

461

462



464

465 Fig 3. Total concentration of copper (ppm) in healthy mouse brain in function of age. Boxes extend  
 466 from the 25<sup>th</sup> and 75<sup>th</sup> percentile, the line inside the box represents the median, the whiskers show the  
 467 minimum and maximum of the values. p-value < 0.02, \*. GraphPad Prism.

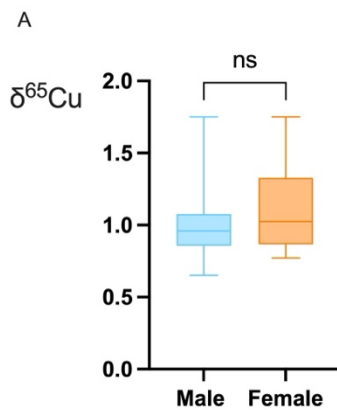
468

469

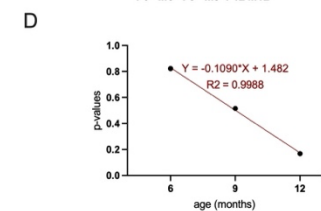
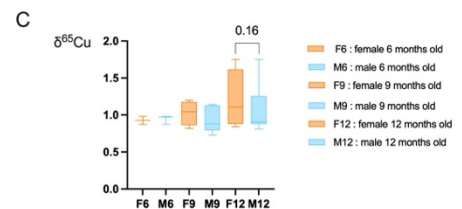
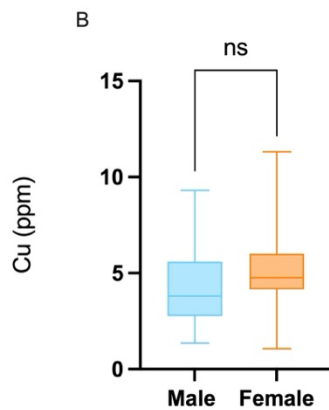
470

471

472



473



474

475

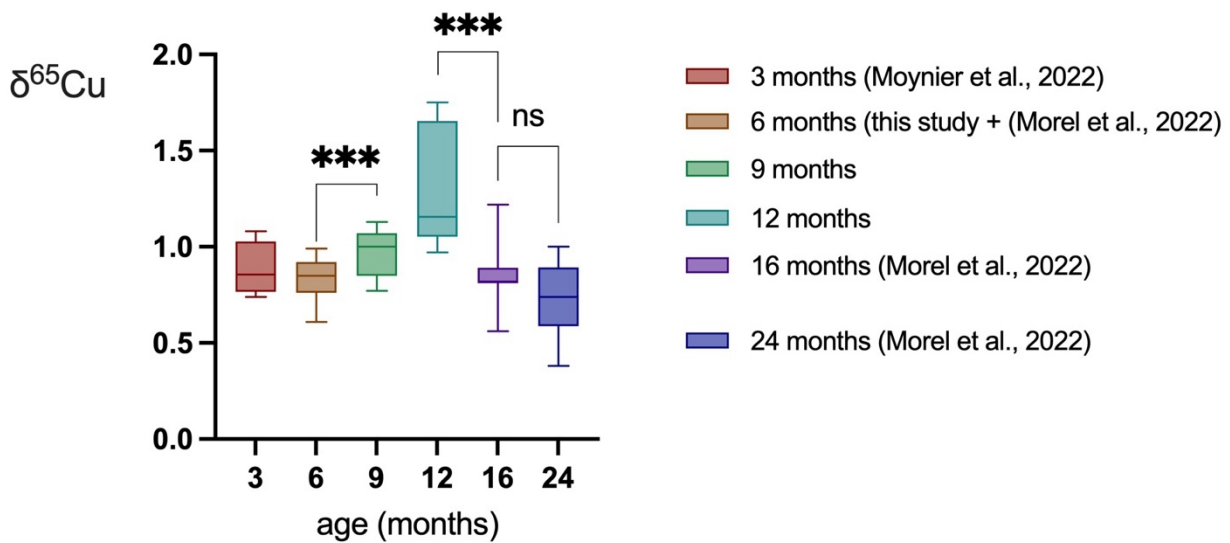
476

477 Fig 4. A, B, C, D.  $\delta^{65}\text{Cu}$  in healthy mouse brain in function of sex (A), copper concentration in  
478 healthy mouse brain in function of sex (B),  $\delta^{65}\text{Cu}$  in healthy mouse brain in function of sex and age,  
479 p-value = 0.16, non-significative (C). (D) is the evolution of the p-values for unpaired-t tests between  
480 males and females as a function of age,  $R^2 = 0.9988$ . Boxes extend from the 25<sup>th</sup> and 75<sup>th</sup> percentile,  
481 the line inside the box represents the median, the whiskers show the minimum and maximum of the  
482 values. ns: not significative.

483

484

485



486

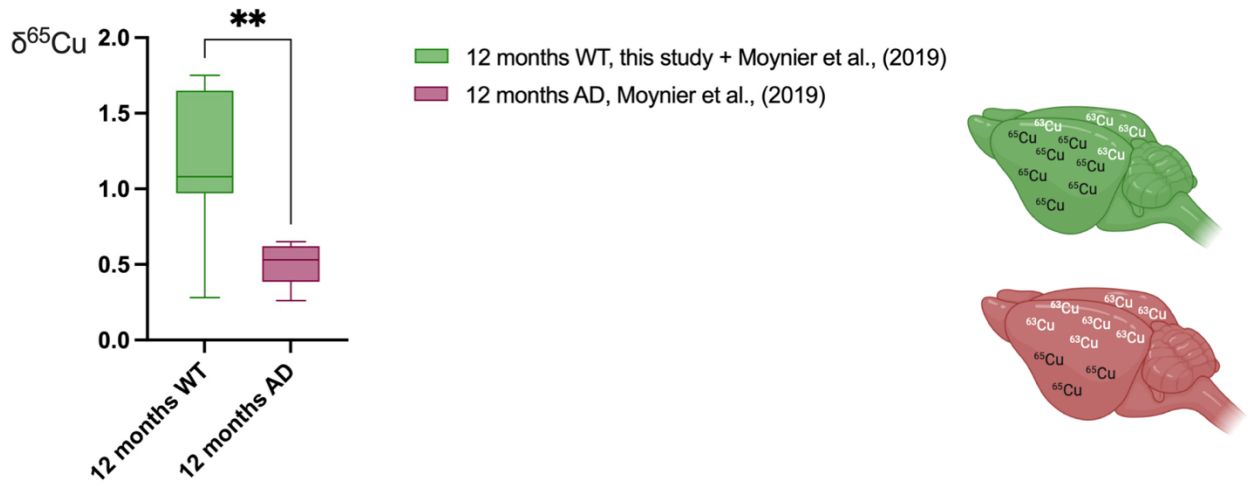
487

488 Fig5.  $\delta^{65}\text{Cu}$  in healthy mouse brain in function of age. Data from (Moynier et al., 2022) and (Morel  
489 et al., 2022) were incorporated to the data from this study. Boxes extend from the 25<sup>th</sup> and 75<sup>th</sup>  
490 percentile, the line inside the box represents the median, the whiskers show the minimum and  
491 maximum of the values. p-value < 0.001, \*\*\*. GraphPad Prism.

492

493

494



495

496

497

498

499

500 Fig 6. A, B. Isotopic composition of copper in the brain of healthy and AD mice. p-value < 0.001, \*\*  
501 (A), copper isotopic composition of a healthy (green) and Alzheimer brain (red) (B). Boxes extend  
502 from the 25<sup>th</sup> and 75<sup>th</sup> percentile, the line inside the box represents the median, the whiskers show the  
503 minimum and maximum of the values. GraphPad Prism, Bio Render.

504

505

506

507

508

509

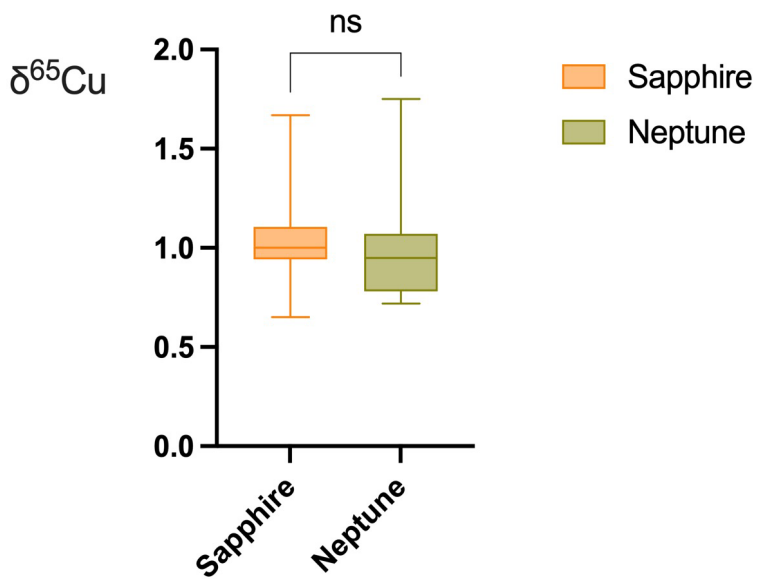
510

511

512

513

514



515

516 **FigS1.** Copper isotopic composition of healthy mice brains depending on the MC-ICP-MS used for  
517 the measure. ns = not significant. GraphPad Prism.

518

519

520

## 521 **References**

- 522 1. McLean, C. A., Cherny, R. A., Fraser, F. W., Fuller, S. J., Smith, M. J., Beyreuther, K., Bush,  
523 A. I., Masters, C. L. Soluble pool of Abeta amyloid as a determinant of severity of  
524 neurodegeneration in Alzheimer's disease. *Ann. Neurol*, 1999, 46, 860–866. doi: 10.1002/1531-  
525 8249(199912)46:6<860::aid-ana8>3.0.co;2-m

526

- 527 2. Mattson, MP., Arumugam, TV. Hallmarks of brain aging: adaptive and pathological  
528 modification by metabolic states. *Cell. Metab*, 2018, 27, 1176-1199. doi:  
529 10.1016/j.cmet.2018.05.011.
- 530  
531
- 532 3. Junqueira VB, Barros SB, Chan SS, Rodrigues L, Giavarotti L, Abud RL, Deucher GP. Aging  
533 and oxidative stress. *Mol. Aspects. Med.*, 2004, 5-16. doi: 10.1016/j.mam.2004.02.003.
- 534 4. Harman, D. Protein oxidation in aging and age-related diseases. *Gerontology*, 1956, 11, 298-  
535 300. doi:10.1093/geronj/11.3.298.
- 536
- 537 5. Harman, D. The biologic clock: the mitochondria? *J. Am. Geriatr. Soc.*, 1972, 4,145-7.  
538 doi:10.1111/j.1532-5415.1972.tb00787.x.
- 539
- 540 6. Beckman KB, Ames BN. The free radical theory of aging matures. *Physiol Rev*, 1998, 78, 547-  
541 81. doi: 10.1152/physrev.1998.78.2.547.
- 542
- 543 7. Berr, C., Balansard, B., Arnaud, J., Roussel, AM., Alperovitch, A. Cognitive Decline Is  
544 Associated with Systemic Oxidative Stress: The EVA Study. *J Am Geriatr Soc*, 2000, 48, 1285-  
545 1291. doi: 10.1111/j.1532-5415.2000.tb02603.x.
- 546  
547
- 548 8. Gemechu, JM., Bentivoglio, M., T cell recruitment in the brain during normal aging. *Front. Cell.*  
549 *Neurosci.*, 2012, 6, 38. doi: 10.3389/fncel.2012.00038.
- 550
- 551 9. Deleidi, M., Jäggle, M., Rubino, G. Immune aging, dysmetabolism, and inflammation in  
552 neurological diseases. *Front. Neurosci.*, 2015, 9, 172. doi: 10.3389/fnins.2015.00172.
- 553

- 554 10. Kempuraj, D., Thangavel, R., Natteru, PA., Selvakumar, G. P., Saeed, D., Zahoor, H., Zaheer,  
555 A. Neuroinflammation induces neurodegeneration. *J. Neurosurg.: Spine.*, 2016, 1.  
556  
557
- 558 11. Roberts, BR., Ryan, TM., Bush, AI., Masters, CL., Duce, JA. The role of metallobiology and  
559 amyloid -  $\beta$  peptides in Alzheimer's disease. *J. Neurochem.*, 2012, 120, 149-166. doi:  
560 10.1111/j.1471-4159.2011.07500.x.  
561
- 562 12. Knopman, DS., Amieva, H., Petersen, RC. Alzheimer disease. *Nat. Rev. Dis. Primers.*, 2021,  
563 7, 33 2021. doi: 10.1038/s41572-021-00269-y  
564
- 565 13. Prince, MJ., Wimo, A., Guerchet, MM., Ali, GC., Wu, YT., Prina, M. World Alzheimer Report  
566 2015-The Global Impact of Dementia: An analysis of prevalence, incidence, cost and trends.  
567 2015.
- 568 14. Hampel, H., Hardy, J., Blennow, K. The Amyloid- $\beta$  Pathway in Alzheimer's Disease. *Mol.*  
569 *Psychiatry.*, 2021, 26, 5481–5503. doi: 10.1038/s41380-021-01249-0  
570
- 571 15. Mucke, L., Selkoe, DJ. Neurotoxicity of amyloid  $\beta$ -protein: synaptic and network dysfunction.  
572 *Cold Spring Harb. Perspect. Med.* , 2012, 2, a006338. doi: 10.1101/cshperspect.a006338.  
573
- 574 16. Hardy, JA., Higgins, GA. Alzheimer's disease: the amyloid cascade hypothesis. *Science*, 1992,  
575 256, 184-185. doi: 10.1126/science.1566067  
576  
577
- 578 17. Zempel, H., Mandelkow, E. Lost after translation: missorting of Tau protein and consequences  
579 for Alzheimer disease. *Trends. Neurosci.*, 2014, 37, 721-732. doi: 10.1016/j.tins.2014.08.004.  
580

- 581 18. Gordon, BA., Blazey, TM., Su, Y., Hari-Raj, A., Dincer, A., Flores, S., Benzinger, TL. Spatial  
582 patterns of neuroimaging biomarker change in individuals from families with autosomal  
583 dominant Alzheimer's disease: a longitudinal study. *Lancet. Neurol.*, 2018, 17, 241-250.  
584 doi:10.1016/S1474-4422(18)30028-0.  
585
- 586 19. Blennow, K., Zetterberg, H. Biomarkers for Alzheimer's disease: current status and prospects  
587 for the future. *J. Intern. Med.*, 2018, 284, 643-663. doi: 10.1111/joim.12816.  
588  
589
- 590 20. Olsson, B., Lautner, R., Andreasson, U., Öhrfelt, A., Portelius, E., Bjerke, M., Zetterberg, H.  
591 CSF and blood biomarkers for the diagnosis of Alzheimer's disease: a systematic review and  
592 meta-analysis. *Lancet Neurol.*, 2016, 15, 673-684. doi: 10.1016/S1474-4422(16)00070-3.  
593
- 594 21. Dubois, B., Feldman, HH., Jacova, C., Hampel, H., Molinuevo, JL., Blennow, K. Advancing  
595 research diagnostic criteria for Alzheimer's disease: the IWG-2 criteria. *Lancet. Neurol.*, 2014,  
596 13, 614–29. doi: 10.1016/S1474-4422(14)70155-3.  
597
- 598 22. Faa, G., Lisci, M., Caria, M. P., Ambu, R., Sciota, R., Nurchi, V. M., Crisponi, G. Brain copper,  
599 iron, magnesium, zinc, calcium, sulfur and phosphorus storage in Wilson's disease. *J. Trace  
600 Elem Med. Biol.*, 2001, 15, 155-160. doi: 10.1016/S0946-672X(01)80060-2.  
601  
602
- 603 23. Nooijen, JL., De Groot, CJ., Van Den Hamer, CJ., Monnens, LA., Willemsse, J., Niermeijer, MF.  
604 Trace element studies in three patients and a fetus with Menkes' disease. Effect of copper  
605 therapy. *Pediatr. Res.*, 1981, 15, 284-289. doi: 10.1203/00006450-198103000-00017.  
606

- 607 24. Sauzéat L, Bernard E, Perret-Liaudet A, Quadrio I, Vighetto A, Krolak-Salmon P, Broussolle  
608 E, Leblanc P, Balter V. Isotopic Evidence for Disrupted Copper Metabolism in Amyotrophic  
609 Lateral Sclerosis. *iScience*, 2018, 6, 264-271. doi: 10.1016/j.isci.2018.07.023.
- 610  
611
- 612 25. Barnham KJ., Bush AI. Biological metals and metal-targeting compounds in major  
613 neurodegenerative diseases. *Chem. Soc. Rev*, 2014, 43, 6727–6749. doi : 10.1039/C4CS00138A
- 614
- 615 26. Pithadia, AS., Lim, MH. Metal-associated amyloid- $\beta$  species in Alzheimer's disease. *Curr. Opin.*  
616 *Chem. Biol.*, 2012, 16, 67-73. doi: 10.1016/j.cbpa.2012.01.016.
- 617
- 618 27. Moynier, F., Vance, D., Fujii, T., Savage, P. The isotope geochemistry of zinc and copper. *Rev.*  
619 *Mineral. Geochem.*, 2017, 82, 543-600. doi:10.2138/rmg.2017.82.13.
- 620
- 621 28. Moynier, F., Creech, J., Dallas, J., Le Borgne, M. Serum and brain natural copper stable isotopes  
622 in a mouse model of Alzheimer's disease. *Sci. Rep.*, 2019, 9, 11894. doi : 10.1038/s41598-019-  
623 47790-5.
- 624
- 625 29. Scheiber, IF., Dringen, R. Astrocyte functions in the copper homeostasis of the brain.  
626 *Neurochem. Int.*, 2013, 62, 556-565. doi: 10.1016/j.neuint.2012.08.017.
- 627  
628
- 629 30. Kaim, W., Rall, J. Copper—a “modern” bioelement. *Angewandte Chemie International Edition*  
630 *in English*, 1996, 35, 43-60. doi: 10.1002/anie.199600431.
- 631

- 632 31. Rubino, JT., Franz, KJ. Coordination chemistry of copper proteins: how nature handles a toxic  
633 cargo for essential function. *J. Inorg. Biochem.*, 2012, 107, 129-143. doi:  
634 10.1016/j.jinorgbio.2011.11.024.
- 635
- 636 32. Atwood, CS., Scarpa, RC., Huang, X., Moir, RD., Jones, WD., Fairlie, DP., Bush, AI.  
637 Characterization of Copper Interactions with Alzheimer Amyloid  $\beta$  Peptides: Identification of  
638 an Attomolar-Affinity Copper Binding Site on Amyloid  $\beta$ 1-42. *J. Neurochem*, 2000, 75, 1219-  
639 1233. doi: 10.1046/j.1471-4159.2000.0751219.
- 640
- 641 33. Conforti, A., Franco, L., Milanino, R., Totorizzo, A., Velo, GP. Copper metabolism during acute  
642 inflammation: studies on liver and serum copper concentrations in normal and inflamed rats. *Br.*  
643 *J. Pharmacol.*, 1983, 79, 45. doi: 10.1111/j.1476-5381.1983.tb10493.x.
- 644
- 645 34. Lech, T., Sadlik, JK. Copper concentration in body tissues and fluids in normal subjects of  
646 southern Poland. *Biol. Trace. Elem. Res.*, 2007, 118, 10-15. doi:10.1007/s12011-007-0014-z.
- 647
- 648
- 649 35. Rahil-Khazen, R., Bolann, BJ., Myking, A., Ulvik, RJ. Multi-element analysis of trace element  
650 levels in human autopsy tissues by using inductively coupled atomic emission spectrometry  
651 technique (ICP-AES). *J. Trace Elem. Med. Biol.*, 2002, 16, 15-25. doi: 10.1016/S0946-  
652 672X(02)80004-9.
- 653
- 654 36. Wong, PC., Waggoner, D., Subramaniam, JR., Tessarollo, L., Bartnikas, TB., Culotta, VC.,  
655 Gitlin, JD. Copper chaperone for superoxide dismutase is essential to activate mammalian  
656 Cu/Zn superoxide dismutase. *Proc. Natl. Acad. Sci. U.S.A.*, 2000, 97, 2886-2891. doi:  
657 org/10.1073/pnas.040461197

658

659 37. Mahan, B., Moynier, F., Jørgensen, AL., Habekost, M., Siebert, J. Examining the homeostatic  
660 distribution of metals and Zn isotopes in Göttingen minipigs. *Metallomics*, 2018, 10, 1264-1281.  
661 doi : 10.1039/c8mt00179k.

662

663 38. Fujii, T., Moynier, F., Abe, M., Nemoto, K., Albarède, F. Copper isotope fractionation between  
664 aqueous compounds relevant to low temperature geochemistry and biology. *Geochim.*  
665 *Cosmochim. Acta.*, 2013, 110, 29-44. doi: 10.1016/j.gca.2013.02.007.

666

667 39. Paquet, M., Fujii, T., Moynier, F. Copper isotope composition of hemocyanin. *J. Trace Elem.*  
668 *Med. Biol.*, 2022, 71, 126967. doi: 10.1016/j.jtemb.2022.126967.

669

670 40. Mahan, B., Antonelli, M. A., Burckel, P., Turner, S., Chung, R., Habekost, M., Moynier, F.  
671 Longitudinal biometal accumulation and Ca isotope composition of the Göttingen minipig  
672 brain. *Metallomics*, 2020, 12, 1585-1598.

673

674

675 41. Albarede, F., Télouk, P., Balter, V., Bondanese, VP., Albalat, E., Oger, P., Fujii, T. Medical  
676 applications of Cu, Zn, and S isotope effects. *Metallomics*, 2016, 8, 1056-1070. doi:  
677 10.1039/c5mt00316d

678

679 42. Moynier, F., Borgne, M. L., Lahoud, E., Mahan, B., Mouton-Liger, F., Hugon, J., Paquet, C.  
680 Copper and zinc isotopic excursions in the human brain affected by Alzheimer's disease.  
681 *Alzheimer's. Dement.: Diagn. Assess. Dis.*, 2020, 12, e12112. doi:10.1002/dad2.12112.

682

- 683 43. Moynier, F., Merland, A., Rigoussen, D., Moureau, J., Paquet, M., Mahan, B., Le Borgne, M.  
684 Baseline distribution of stable copper isotope compositions of the brain and other organs in mice.  
685 *Metallomics*, 2022, 14. doi:10.1093/mtomcs/mfac017.  
686
- 687 44. Moynier, F., Fujii, T. Theoretical isotopic fractionation of magnesium between chlorophylls.  
688 *Sci. Rep.*, 2017, 7, 6973. doi: 10.1038/s41598-017-07305-6.  
689
- 690 45. Schauble, EA. Applying stable isotope fractionation theory to new systems. *Rev. Mineral.*  
691 *Geochem.*, 2004, 55, 65-111. doi: 10.2138/gsrmg.55.1.65.  
692
- 693 46. Balter, V., Nogueira da Costa, A., Bondanese, V. P., Jaouen, K., Lamboux, A., Sangrajrang, S.,  
694 Hainaut, P. Natural variations of copper and sulfur stable isotopes in blood of hepatocellular  
695 carcinoma patients. *Proc. Natl. Acad. Sci*, 2015, U.S.A, 112, 982-985. doi:  
696 10.1073/pnas.1415151112  
697
- 698 47. Télouk P, Puisieux A, Fujii T, Balter V, Bondanese VP, Morel AP, Clapisson G, Lamboux A,  
699 Albarede F. Copper isotope effect in serum of cancer patients. A pilot study. *Metallomics*, 2015,  
700 299-308. doi: 10.1039/c4mt00269e.  
701  
702
- 703 48. Schilling, K., Larnier, F., Saad, A., Roberts, R., Kocher, H. M., Blyuss, O., Crnogorac-Jurcevic,  
704 T. Urine metallomics signature as an indicator of pancreatic cancer. *Metallomics*, 2020, 12, 752-  
705 757 doi: 10.1039/d0mt00061b  
706
- 707 49. Schilling, K., Moore, R. E., Capper, M. S., Rehkämper, M., Goddard, K., Ion, C., Larnier, F.  
708 Zinc stable isotopes in urine as diagnostic for cancer of secretory organs. *Metallomics*, 2021,  
709 13, mfab020. doi: 10.1093/mtomcs/mfab020

710

711

712 50. Costa-Rodríguez, M., Anoushkina, Y., Lauwens, S., Van Vlierberghe, H., Delanghe, J.,  
713 Vanhaecke, F. Isotopic analysis of Cu in blood serum by multi-collector ICP-mass spectrometry:  
714 A new approach for the diagnosis and prognosis of liver cirrhosis? *Metallomics*, 2015, 7, 491–  
715 498. doi:10.1039/c4mt00319e.

716

717 51. Costas-Rodríguez, M., Van Campenhout, S., Hastuti, AA., Devisscher, L., Van Vlierberghe, H.,  
718 Vanhaecke, F. Body distribution of stable copper isotopes during the progression of cholestatic  
719 liver disease induced by common bile duct ligation in mice. *Metallomics*, 2019, 11, 1093-1103.  
720 doi:10.1039/c8mt00362a.

721

722

723 52. Lamboux, A., Couchonnal-Bedoya, E., Guillaud, O., Laurencin, C., Lion-François, L.,  
724 Belmalih, A., Balter, V. The blood copper isotopic composition is a prognostic indicator of the  
725 hepatic injury in Wilson disease. *Metallomics*, 2020, 12, 1781-1790. doi:10.1039/d0mt00167h.

726

727 53. Lauwens, S., Costas-Rodríguez, M., Van Vlierberghe, H., Vanhaecke, F. Cu isotopic signature  
728 in blood serum of liver transplant patients: a follow-up study. *Sci. Rep.*, 2016, 6, 30683. doi:  
729 10.1038/srep30683.

730

731 54. Van Campenhout, S., Hastuti, AA., Lefere, S., Van Vlierberghe, H., Vanhaecke, F., Costas-  
732 Rodríguez, M., Devisscher, L. Lighter serum copper isotopic composition in patients with early  
733 non-alcoholic fatty liver disease. *BMC Research Notes*, 2020, 13, 225. doi: 10.1186/s13104-  
734 020-05069-3.

735

- 736 55. Lerner, AJ. MACE for diagnosis of dementia and MCI: examining cut-offs and predictive  
737 values. *Diagnostics*, 2019, 9, 51. doi: 10.3390/diagnostics9020051.
- 738
- 739 56. Solovyev, N., El-Khatib, A. H., Costas-Rodríguez, M., Schwab, K., Griffin, E., Raab, A.,  
740 Vanhaecke, F. Cu, Fe, and Zn isotope ratios in murine Alzheimer's disease models suggest  
741 specific signatures of amyloidogenesis and tauopathy. *J. Biol. Chem.*, 2021, 296. doi :  
742 10.1016/j.jbc.2021.100292.
- 743
- 744 57. Tõugu, V, Tiiman, A, Palumaa, P. Interactions of Zn(ii) and Cu(ii) ions with Alzheimer's  
745 amyloid-beta peptide. Metal ion binding, contribution to fibrillization and toxicity. *Metallomics*,  
746 2011, 3, 250–. doi:10.1039/c0mt00073f
- 747
- 748
- 749 58. Zhao, J., Shi, Q., Tian, H., Li, Y., Liu, Y., Xu, Z., Meunier, B. TDMQ20, a specific copper  
750 chelator, reduces memory impairments in Alzheimer's disease mouse models. *ACS Chem.*  
751 *Neurosci.*, 2020, 12, 140-149. doi: 10.1021/acchemneuro.0c00621.
- 752
- 753 59. Sarell, CJ., Syme, CD., Rigby, SE., Viles, JH. Copper (II) binding to amyloid- $\beta$  fibrils of  
754 Alzheimer's disease reveals a picomolar affinity: stoichiometry and coordination geometry are  
755 independent of A $\beta$  oligomeric form. *Biochemistry*, 2009, 48, 4388-4402. doi:  
756 10.1021/bi900254n.
- 757
- 758 60. Barritt, JD., Viles, JH. Truncated amyloid- $\beta$  (11–40/42) from Alzheimer disease binds Cu<sup>2+</sup>  
759 with a femtomolar affinity and influences fiber assembly. *J. Biol. Chem*, 2015, 290, 27791-  
760 27802. doi: 10.1074/jbc.M115.684084

761  
762

- 763 61. Drew, SC. The case for abandoning therapeutic chelation of copper ions in Alzheimer's Disease.  
764 Front. Neurosci., 2017, 11, 317. doi: 10.3389/fnins.2017.00317  
765
- 766 62. Mital, M., Wezynfeld, NE., Frączyk, T., Wiloch, MZ., Wawrzyniak, UE., Bonna, A., Drew, SC.  
767 A functional role for A $\beta$  in metal homeostasis? N-truncation and high-affinity copper binding.  
768 Angew. Chem., 2015, 127, 10606-10610. doi: 10.1002/ange.201502644.  
769  
770
- 771 63. Dai, B., Sargent, CJ., Gui, X., Liu, C., Zhang, F. Fibril self-assembly of amyloid–spider silk  
772 block polypeptides. Biomacromolecules, 2019, 20, 2015-2023. doi:  
773 10.1021/acs.biomac.9b00218.  
774
- 775 64. Strozyk, D., Launer, LJ., Adlard, PA., Cherny, RA., Tsatsanis, A., Volitakis, I., Bush, AI. 2009.  
776 Zinc and copper modulate Alzheimer A $\beta$  levels in human cerebrospinal fluid. Neurobiol.  
777 Aging., 30, 1069-1077. doi:10.1016/j.neurobiolaging.2007.10.012.  
778  
779
- 780 65. Maréchal, CN., Télouk, P., Albarède, F. Precise analysis of copper and zinc isotopic  
781 compositions by plasma-source mass spectrometry. Chem. Geol., 1999, 156, 251-273. doi:  
782 10.1016/S0009-2541(98)00191-0  
783
- 784 66. Sauzéat, Marta Costas-Rodríguez, Emmanuelle Albalat, Nadine Mattielli, Frank  
785 Vanhaecke, Vincent Balter, Inter-comparison of stable iron, copper and zinc isotopic  
786 compositions in six reference materials of biological origin, Talanta, 2021, 221, 121-576. doi:  
787 10.1016/j.talanta.2020.121576.  
788

- 789 67. Maynard, CJ., Cappai, R., Volitakis, I., Cherny, RA., White, AR., Beyreuther, K., Li, QX.  
790 Overexpression of Alzheimer's disease amyloid- $\beta$  opposes the age-dependent elevations of brain  
791 copper and iron. *J. Biol. Chem.*, 2002, 277, 44670-44676. doi: 10.1074/jbc.M204379200.  
792
- 793 68. Madaric, A., Ginter, E., Kadrabova, J. Serum copper, zinc and copper/zinc ratio in males:  
794 influence of aging. *Physiol. Res.*, 1994, 43, 107-107.  
795
- 796 69. Deibel, MA., Ehmann, WD., Markesbery, WR. Copper, iron, and zinc imbalances in severely  
797 degenerated brain regions in Alzheimer's disease: possible relation to oxidative stress. *J. Neurol.*  
798 *Sci.*, 1996, 143, 137-142. doi: 10.1016/S0022-510X(96)00203-1.  
799
- 800 70. Miller, LM., Wang, Q., Telivala, TP., Smith, RJ., Lanzirotti, A., Miklossy, J. Synchrotron-based  
801 infrared and X-ray imaging shows focalized accumulation of Cu and Zn co-localized with  $\beta$ -  
802 amyloid deposits in Alzheimer's disease. *J. Struct. Biol.*, 2006, 155, 30-37. doi:  
803 10.1016/j.jsb.2005.09.004.  
804  
805
- 806 71. Bales, CW., Freeland-Graves, JH., Askey, S., Behmardi, F., Pobocik, RS., Fickel, JJ., Greenlee,  
807 P. Zinc, magnesium, copper, and protein concentrations in human saliva: age-and sex-related  
808 differences. *Am. J. Clin. Nutr.*, 1990, 51, 462-469. doi: 10.1093/ajcn/51.3.46.  
809
- 810 72. Palm R, Wahlström G, Hallmans G. Age related changes in weight and the concentrations of  
811 zinc and copper in the brain of the adult rat. *Lab. Anim.*, 1990, 24, 240-245.  
812 doi:10.1258/002367790780866128  
813
- 814 73. Albarède, F. Metal stable isotopes in the human body: a tribute of geochemistry to medicine.  
815 *Elements*, 2015, 11, 265-269. doi: 10.2113/gselements.11.4.265

816

817

818 74. Jaouen K., Balter V., Herrscher E., Lamboux A., Télouk P., Albarède F. Fe and Cu stable  
819 isotopes in archeological human bones and their relationship to sex. *Am. J. Phys. Anthropol.*,  
820 2012, 148:334–340. doi: 10.1002/ajpa.22053.

821

822 75. Van Den Eeden SK, Tanner CM, Bernstein AL, Fross RD, Leimpeter A, Bloch DA, Nelson LM.  
823 Incidence of Parkinson's disease: variation by age, gender, and race/ethnicity. *Am. J. Epidemiol.*  
824 2003, 157, 1015-22. doi: 10.1093/aje/kwg068.

825

826

827 76. Wooten GF, Currie LJ, Bovbjerg VE, Lee JK, Patrie J. Are men at greater risk for Parkinson's  
828 disease than women? *J. Neurol. Neurosurg. Psychiatry.*, 2004, 637-9. doi:  
829 10.1136/jnnp.2003.020982.

830

831 77. Shulman, A., Goldstein, B., Strashun, A. M. Central nervous system neurodegeneration and  
832 tinnitus: a clinical experience. *Int Tinnitus J*, 2007, 13, 118-31.

833

834 78. Hebert LE, Weuve J, Scherr PA, Evans DA. Alzheimer disease in the United States (2010-2050)  
835 estimated using the 2010 census. *Neurology*, 2013, 80, 1778-83. doi:  
836 10.1212/WNL.0b013e31828726f5.

837

838 79. Lapane, KL., Gambassi, G., Landi, F., Sgadari, A., Mor, V., Bernabei, R. Gender differences in  
839 predictors of mortality in nursing home residents with AD. *Neurology*, 2001, 56, 650-654.  
840 doi:10.1212/WNL.56.5.650.

841

- 842 80. Everett, J., Lermyte, F., Brooks, J., Tjendana-Tjhin, V., Plascencia-Villa, G., Hands-Portman, I,  
843 Telling, N. D. Biogenic metallic elements in the human brain? *Sci. Adv.*, 2021, 7, eabf6707.  
844 doi: 10.1126/sciadv.abf6707.
- 845  
846 81. Giacoppo, S., Mandolino, G., Galuppo, M., Bramanti, P., Mazzon, E. Cannabinoids: new  
847 promising agents in the treatment of neurological diseases. *Molecules*, 2014, 19, 18781-18816.  
848 doi : 10.3390/molecules191118781.
- 849  
850 82. Klevay, LM. Alzheimer's disease as copper deficiency. *Med. Hypotheses.*, 2008, 70, 802-807.  
851 doi: 10.1016/j.mehy.2007.04.051
- 852  
853 83. Exley, C., House, E., Polwart, A., Esiri, MM. Brain burdens of aluminum, iron, and copper and  
854 their relationships with amyloid- $\beta$  pathology in 60 human brains. *J. Alzheimer's Dis.*, 2012, 31,  
855 725-730. doi: 10.3233/JAD-2012-120766.
- 856  
857 84. Hung YH, Bush AI, La Fontaine S. Links between copper and cholesterol in Alzheimer's  
858 disease. *Front. Physiol.*, 2013, 4-111. doi: 10.3389/fphys.2013.00111
- 859  
860  
861  
862 85. Abreu IA, Cabelli DE. Superoxide dismutases-a review of the metal-associated mechanistic  
863 variations. *Biochim Biophys Acta.* 2010, 263-74. doi: 10.1016/j.bbapap.2009.11.005. Epub  
864 2009 Nov 13. PMID: 19914406.
- 865  
866  
867 86. Fukai, T., Ushio-Fukai, M. Superoxide dismutases: role in redox signaling, vascular function,  
868 and diseases. *Antioxid Redox Signal.*, 2011, 15, 1583-606. doi: 10.1089/ars.2011.3999.
- 869

- 870 87. Crapo, JD., Oury, T., Rabouille, C., Slot, JW., Chang, LY. Copper, zinc superoxide dismutase  
871 is primarily a cytosolic protein in human cells. Proc. Natl. Acad. Sci. U S A, 1992, 89, 10405-  
872 9. doi: 10.1073/pnas.89.21.10405.
- 873  
874 88. Okado-Matsumoto A., Fridovich I. Subcellular distribution of superoxide dismutases (SOD) in  
875 rat liver: Cu,Zn-SOD in mitochondria. J. Biol. Chem., 2001, 276, 38388-93. doi:  
876 10.1074/jbc.M105395200.
- 877  
878
- 879 89. Warner, HR. Superoxide dismutase, aging, and degenerative disease. Free. Radic. Biol. Med.,  
880 1994, 17, 249-258. doi: 10.1016/0891-5849(94)90080-9
- 881
- 882 90. Larner, F., McLean, CA., Halliday, A., Blaine R. Copper Isotope Compositions of Superoxide  
883 Dismutase and Metallothionein from Post-Mortem Human Frontal Cortex. Inorganics, 2019, 7,  
884 86-. doi:10.3390/inorganics7070086
- 885  
886
- 887 91. Rybka J, Kupczyk D, Kędziora-Kornatowska K, et al. Glutathione-related antioxidant defense  
888 system in elderly patients treated for hypertension. Cardiovasc. Toxicol., 2011, 1-9. doi:  
889 10.1007/s12012-010-9096-5.
- 890
- 891 92. Parpura V., Heneka M. T., Montana V., Oliet S. H., Schousboe A., Haydon PG., Glial cells in  
892 (patho)physiology. J. Neurochem., 2012, 121, 4–27. doi: 10.1111/j.1471-4159.2012.07664.x
- 893
- 894 93. Schmidt, MM., Dringen, R. Glutathione (GSH) synthesis and metabolism. Neur. Met. in vivo,  
895 2012, 1029-1050. doi: 10.1007/978-1-4614-1788-0\_36.
- 896  
897

- 898 94. Dringen, R., Bishop, GM., Koeppe, M., Dang, TN., Robinson, SR. The pivotal role of astrocytes  
899 in the metabolism of iron in the brain. *Neurochem. Res*, 2007, 32, 1884–1890. doi:  
900 10.1007/s11064-007-9375-0  
901
- 902 95. Tiffany-Castiglioni, E., Hong, S., Qian, Y. Copper handling by astrocytes: insights into  
903 neurodegenerative diseases. *Int. J. Dev. Neurosci.*, 2011, 29, 811-818. doi:  
904 10.1016/j.ijdevneu.2011.09.004  
905  
906
- 907 96. Dringen, R., Scheiber, IF., Mercer, JF. Copper metabolism of astrocytes. *Front. Aging.*  
908 *Neurosci.*, 2013, 5, 9. doi: 10.3389/fnagi.2013.00009.
- 909 97. Scheiber IF., Mercer JF., Dringen R. 2010. Copper accumulation by cultured astrocytes.  
910 *Neurochem. Int*, 451-60. doi: 10.1016/j.neuint.2009.12.002.  
911
- 912 98. Aschner M., Astrocyte metallothioneins (MTs) and their neuroprotective role. *Ann.N.*  
913 *Y.Acad.Sci.* 1997, 825, 334-347. doi: 10.1111/j.1749-6632.1997.tb48445.x  
914
- 915 99. Dringen, R., Hamprecht, B. Glutathione restoration as indicator for cellular metabolism of  
916 astroglial cells. *Dev. Neurosci*, 1998, 20, 401-7. doi: 10.1159/000017337.
- 917  
918 100. Lee, J., Pena, M. M. O., Nose, Y., Thiele, D. J. Biochemical characterization of the human  
919 copper transporter Ctr1. *J. Biol. Chem.*, 2002, 277, 4380-4387. doi: 10.1074/jbc.M104728200  
920  
921
- 922 101. Sikora, E., Bielak-Zmijewska, A., Dudkowska, M., Krzystyniak, A., Mosieniak, G.,  
923 Wesierska, M., Włodarczyk, J. Cellular senescence in brain aging. *Front. Aging. Neurosci.*,  
924 2021, 13, 646924. doi: 10.3389/fnagi.2021.646924.  
925

- 926 102. Bhat R., Crowe EP., Bitto A., Moh M., Katsetos CD., Garcia FU., Astrocyte Senescence as a  
927 Component of Alzheimer's Disease. PLoS ONE 7, 2012, e45069. doi :  
928 10.1371/journal.pone.0045069
- 929  
930
- 931 103. Han, X., Zhang, T., Liu, H., Mi, Y., Gou, X. Astrocyte senescence and Alzheimer's disease:  
932 A review. Front. Aging. Neurosci., 2020, 12, 148. doi:10.3389/fnagi.2020.00148.
- 933
- 934 104. Zhou, Q., Zhang, Y., Lu, L., Zhang, H., Zhao, C., Pu, Y., Yin, L. Copper induces microglia-  
935 mediated neuroinflammation through ROS/NF- $\kappa$ B pathway and mitophagy disorder. Food.  
936 Chem. Toxicol., 2022, 168, 113-369. doi : 10.1016/j.fct.2022.113369.
- 937
- 938 105. Nayak, D., Roth, TL., McGavern, DB. Microglia development and function. Annu. Rev.  
939 Immunol., 2014, 32, 367–402. doi:10.1146/annurev-immunol-032713-120240
- 940
- 941 106. Ashraf, A., Michaelides, C., Walker, TA., Ekonomou, A., Suessmilch, M., Sriskanthanathan,  
942 A., So, PW. Regional distributions of iron, copper and zinc and their relationships with glia in a  
943 normal aging mouse model. Front. Aging. Neurosci, 2019, 351. doi: 10.3389/fnagi.2019.00351
- 944
- 945 107. Morel, JD., Sauzéat, L., Goeminne, L.J.E. et al. The mouse metallomic landscape of aging  
946 and metabolism. Nat Commun, 2022, 607. <https://doi.org/10.1038/s41467-022-28060-x>
- 947
- 948 108. World Health Organization, Dementia, Key facts, 2015, [https://www.who.int/news-](https://www.who.int/news-room/fact-sheets/detail/dementia)  
949 [room/fact-sheets/detail/dementia](https://www.who.int/news-room/fact-sheets/detail/dementia).
- 950
- 951 109. Lamboux, A., Couchonnal, E., Guillaud, O., Laurencin, C., Lion-François, L., Belmalih, A.,  
952 Mintz, E., Brun, V., Bost, M., Lachaux, A., Balter, V., The blood copper isotopic composition

953 is a prognostic indicator of the hepatic injury in Wilson disease, *Metallomics*, 2020, 12.  
954 10.1039/D0MT00167H.

955  
956 110. Aramendía, M., Rello V., Luis Resano, M., Vanhaecke, F. Isotopic analysis of Cu in serum  
957 samples for diagnosis of Wilson's disease: A pilot study 2013. *J. Anal. At. Spectrom.* 675-681.  
958 10.1039/C3JA30349G.

959  
960 111. Frutiger, K., Lukas, T., J., Gorrie, G., et al. Gender difference in levels of Cu/Zn superoxide  
961 dismutase (SOD1) in cerebrospinal fluid of patients with amyotrophic lateral sclerosis.  
962 2008 *Amyotrophic Lateral Sclerosis*, 184-187. 10.1080/17482960801984358

963  
964 112. Mahan, B., et al. Isotope metallomics approaches for medical research. *Cell Mol Life Sci*, 77,  
965 2020. doi:10.1007/s00018-020-03484-0

966  
967 113. An, Y., Li, S., Huang, X., Chen, X., Shan, H., Zhang M. The Role of Copper Homeostasis in  
968 Brain Disease. *Int J Mol Sci*. 2022, 23. doi:10.3390/ijms232213850

969  
970 114. Huuskonen, MT., Tuo, QZ., Loppi, S, et al. The Copper bis(thiosemicarbazone) Complex  
971  $\text{Cu}^{\text{II}}(\text{atsm})$  Is Protective Against Cerebral Ischemia Through Modulation of the Inflammatory  
972 Milieu. *Neurotherapeutics*. 2017, 14. doi:10.1007/s13311-016-0504-9

973  
974 115. Soon, CPW., Donnelly, PS., Turner, BJ., et al. Diacetylbis(N(4)-methylthiosemicarbazonato)  
975 copper(II) ( $\text{Cu}^{\text{II}}(\text{atsm})$ ) protects against peroxynitrite-induced nitrosative damage and prolongs  
976 survival in amyotrophic lateral sclerosis mouse model. *J Biol Chem*. 2011, 286.  
977 doi:10.1074/jbc.M111.274407

978  
979 116. Luu TH, Peters D, Lahoud E, Gérard Y, Moynier F. Copper Isotope Compositions Measured  
980 Using a Sapphire Dual Path MC-ICPMS with a Collision/Reaction Cell. *Anal Chem*. 2024 Jan  
981 5. doi: 10.1021/acs.analchem.3c05192. Epub ahead of print. PMID: 38179926.

982

983  
984  
985  
986  
987  
988  
989  
990  
991  
992  
993  
994  
995  
996  
997  
998  
999  
1000  
1001  
1002  
1003  
1004  
1005

1006  
1007  
1008  
1009  
1010  
1011  
1012  
1013  
1014  
1015  
1016  
1017  
1018  
1019  
1020  
1021  
1022  
1023  
1024  
1025  
1026  
1027  
1028  
1029

1030

1031

1032

1033

1034

1035

1036

1037

1038

1039

1040

1041

1042

1043

1044

1045

1046

1047

1048

1049

1050

1051

1052

1053

1054

1055

1056

1057

1058

1059

1060